CASL-U-2013-0204-000

Power uprates
and plant life extension

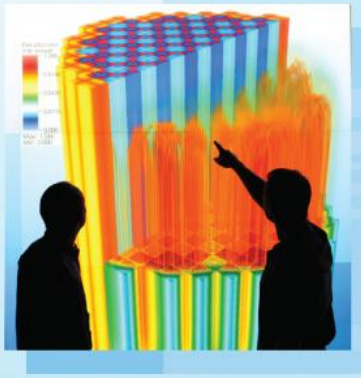

Engineering design
and analysis

Science-enabling
high performance
computing

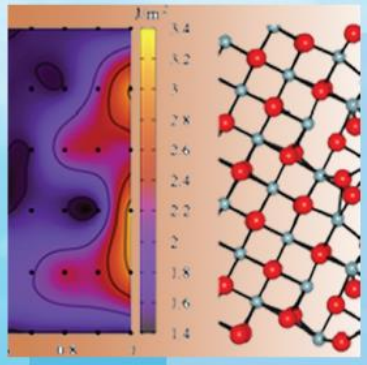

Fundamental science

Plant operational data

Consortium for Advanced Simulation of LWRs

L3:THM.CLS.P7.05
RPI L3 Milestone

Michael Z. Podowski
RPI

August 30, 2013

U.S. DEPARTMENT OF ENERGY | Nuclear Energy

RPI L3 Milestone

Summary of Milestone Accomplishments and Lessons Learned

The RPI L.3 Milestone included two Sub-Milestones or Tasks. A summary of major accomplishments for each Sub-Milestone is given next.

Sub-Milestone 1

Develop a mechanistic CFD model of subcooled boiling applicable to simulate flow and heat transfer in PWR fuel assemblies. Perform numerical testing and validation of the new model using NPHASE-CMFD, prepare model documentation and guidelines for implementation on other CASL multiphase CFD solvers.

Major accomplishments:

- Several new and/or improved mechanistic models of subcooled boiling have been formulated, including the following:
  - Interfacial heat and mass transfer.
  - Vapor generation at heated wall.
  - Condensation-driven bubble collapse in contact with subcooled liquid.
- Individual models have been parametrically tested in a stand-alone fashion.
- New models have been implemented in the NPHASE-CMFD code.
- Calculations have been carried out to test factors affecting numerical consistency and accuracy of simulations.
- Proposed models have been validated against experimental data.
- Subcooled boiling simulations have been performed for prototypical PWR fuel channel geometry and operating conditions.
- The experience gained from the modeling of subcooled boiling at RPI has been shared with CASL partners.

Sub-Milestone 2

Formulate a level-set-based model of simultaneous bubble growth and condensation near the heated wall which is subject to subcooled boiling. The overall objective is to develop, implement in NPHASE-CMFD and test an accurate and efficient method of gas/liquid interface tracking with phase change, and use the new methodology to develop mechanistic closure laws for the RANS model discussed in Sub-Milestone 1.

Major accomplishments:

- Level-set-based interface tracking model method has been developed for vapor bubbles subject to phase change due to thermal non-equilibrium with the surrounding liquid.
- The new model has been numerically implemented in NPASE-CMFD.
- Parametric model testing has been performed for the following conditions:
  - Growth of a flowing bubble in superheated liquid.

- Shrinkage of a flowing bubble in subcooled liquid.
- Simultaneous bubble growth and collapse in a nonuniform liquid temperature field.

❖ Numerical testing of the consistency and accuracy of the proposed computational model have been carried out.

❖ The new model has been applied to simulated subcooled boiling conditions.

❖ Experience gained from the results obtained to date has been used in the development of new models and closure laws for Sub-Milestone 1.

Lessons Learned

❖ The use of theoretical analysis and quasi-analytical solution methods is critical for enhancing our understanding of underlying physical phenomena governing subcooled boiling in nuclear reactors and for reducing the number of adjustable coefficients in the closure laws needed at the RANS modeling level.

❖ A similar conclusion applies to the use of a small scale interface-tracking approach which is capable of capturing the effect of simultaneous evaporation and condensation phase change across variable-temperature liquid field. Such an approach has a great potential to serve as virtual experimental data base for the verification and validation of advanced RANS-type models.

❖ The understanding of the effect of local liquid subcooling near the heated wall on net vapor generation is very important for the predictive capabilities of the overall model.

❖ Phase change (i.e., combined evaporation and condensation) at and near the heated wall may significantly affect the kinematic models governing bubble motion there (such as drag force, lift force and turbulent dispersion force), compared to adiabatic flow conditions.

❖ Accounting for bubble size change due to volumetric condensation in subcooled liquid may have a considerable impact on the predicted void fraction.

❖ The effect of mesh size on the results of two-phase flow simulations is much more complex than for single-phase flows. This is due to the fact that the modeling of turbulent liquid flow and of bubble-liquid interfacial interactions impose different constraints on the near-wall meshing. Using inappropriate meshes may lead to inconsistent and/or incorrect results.

❖ Continuing assistance to other CASL members in the formulation, computer implementation and testing of subcooled boiling models is planned aimed at accelerating the overall progress in the THM milestones.

❖ It is important that further modeling efforts make direct use of new experimental data generated by various members of the THM group.

❖ In addition to the tasks performed according to the current milestones, a preliminary modeling and computational framework have been formulated for two major groups of problems which are considered as some of the most important next steps toward the formulation of the overall model of fluid flow and subcooled boiling heat transfer in PWR reactors:
(a) mechanistic approach to subcooled boiling two-phase flow around spacer grids,
(b) mechanistic models of DNB in PWR fuel assemblies.
The rationale behind the proposed approach is related to the past experience in both areas, as illustrated at the end of this report.

Detailed Report for Sub-Milestone 1

1.1. Interfacial Momentum Transfer

The interfacial momentum transfer model consists of the: drag, virtual mass, turbulent dispersion and lift forces, and also includes terms for momentum transfer due to phase change.
The drag force is formulated as

$$\vec{F}_d = -\frac{3}{4}\frac{C_d}{D_b}\alpha_v \rho_l \left|\vec{u}_v - \vec{u}_l\right|\left(\vec{u}_v - \vec{u}_l\right) \tag{1.1}$$

where D_b is the bubble diameter and α_v is the vapor volume fraction. The drag coefficient is a function of the local relative bubble Reynolds number

$$C_d = \frac{24}{\mathrm{Re}_b}\left(1 + 0.092\,\mathrm{Re}_b^{0.78}\right) \tag{1.2}$$

$$\mathrm{Re}_b = \frac{\rho_l \left|\vec{u}_v - \vec{u}_l\right| D_b}{\mu_l} \tag{1.3}$$

The virtual mass force is expressed as [Drew and Lahey, 1979]

$$\vec{F}_{vm} = -C_{vm}\rho_l \alpha_v \left(\frac{D\vec{u}_v}{Dt} - \frac{D\vec{u}_l}{Dt}\right) \tag{1.4}$$

where the differential operator $D\vec{u}_i / Dt$ represents the material or substantial derivative. The value for the virtual mass coefficient is given as 0.5.
The lift force is modeled as [Drew and Lahey, 1979]

$$\vec{F}_L = -C_L \rho_l \alpha_v \left(\vec{u}_v - \vec{u}_l\right) \times \left(\vec{\nabla} \times \vec{u}_l\right) \tag{1.5}$$

and the turbulent dispersion force is given by Podowski [2009]

$$\vec{F}_{TD} = -C_{TD}\rho_l \alpha_v \underline{\underline{\boldsymbol{\kappa}}}_l \nabla \alpha_v \tag{1.6}$$

where $\underline{\underline{\boldsymbol{\kappa}}}_l = \overline{(u'_{l,i} u'_{l,j})}\delta_{ij}$ for i,j=1,2,3, and δ_{ij} is the Kronecker delta.

It should be noted that for two-phase flows along heated pipes and conduits, Eqs.(1.) and (1.) are valid as long as the distance from the conduit walls is larger than the bubble diameter, i.e. as long as bubble motion is not constrained by the reaction force of the rigid wall. This is consistent with recent modeling work of Jiao and Podowski [2012]. The lift coefficient has been chosen as 0.03, which is also consistent with the formulation provided by Jiao and Podowski [2012].
In addition to the effect of interfacial forces, additional momentum transfer in diabatic flow is due to mass exchange (evaporation and/or condensation) between the vapor and liquid components. The resultant force of fluid component *i* acting on fluid component *j* is accounted for by

$$F_{\Gamma,j} = \sum_{i \neq j}^{I}\left(\Gamma_{i-j}\vec{u}_i - \Gamma_{j-i}\vec{u}_j\right) \tag{1.7}$$

where Γ_{i-j} represents the volumetric rate of mass transfer from field-*i* to field-*j*. The overall kinematic model has been validated before [6] against the experimental data of Wang et al. [1987].

1.2. Interfacial Heat and Mass Transfer

The interfacial heat and mass transfer component assumes that a liquid-vapor interface is present at the saturation temperature. This applies to bubbles which have fully departed from the wall and got dispersed throughout the fluid flow domain. Heat transfer between the interface and each the liquid and vapor bubbles is modeled independently according to

$$q_j''' = N''' A_s H_j \left(T_{sat} - T_j \right) \tag{1.8}$$

where N''' represents the bubble number density, A_s is the bubble surface area, and H_j is the interfacial heat transfer coefficient. The subscript j indicates the individual fluid component, i.e. liquid or vapor. The condensation heat transfer coefficient (interface-to-liquid) is expressed as a function of the bubble relative Reynolds number [Bejan, 2007]

$$Nu = C_{vol} \left[2 + \left(0.4\,\mathrm{Re}_b^{0.5} + 0.06\,\mathrm{Re}_b^{0.66} \right) \mathrm{Pr}_l^{0.4} \right] = \frac{H_l D_b}{k_l} \tag{1.9}$$

The expression given with $C_{vol} = 1$ was originally developed to model heat transfer to a single sphere. For bubbly two-phase flows, the value of C_{vol} is normally greater than one due an enhancement of heat transfer caused by bubble-induced turbulence.

In addition to the heat transfer on the liquid side of the interface, the present model also accounts for heat transfer inside the bubbles (important if bubbles contain superheated vapor). Since the corresponding mechanism is predominantly heat conduction, the approach is based on a rigorous solution to transient conduction in a sphere [Shaver et al, 2010]. The rate of mass transfer is then determined by

$$\Gamma_{v-l} h_{fg} = q_l''' + q_v''' \tag{1.10}$$

where q_v''' is negative for superheated vapor. Extensive testing of the interfacial heat and mass transfer models for various vapor superheats and liquid subcoolings has been performed before [6].

1.3. Vapor Generation

A comprehensive model of wall heat flux partitioning in forced-convection boiling was originally proposed by Kurul and Podowski [1991]. However the model was limited to subcooled boiling. To account for transition from subcooled to saturated boiling, a new approach has been developed and implemented in the current overall model.

In the new proposed model, the wall heat flux has been partitioned into two major components

$$q_w'' = q_b'' + q_{1\phi}'' \tag{1.11}$$

where $q_{1\phi}''$ is the non-boiling (single-phase) component and q_b'' is the boiling component which accounts for both evaporation and quenching. The single phase and boiling heat flux components are respectively given by

$$q_{1\phi} = H_{1\phi} \left(1 - A_b'' \right) \left(\Delta T_w - \Delta T_l \right) \tag{1.12}$$

$$q_b'' = A_b'' \frac{h_{\mathrm{lg}}}{h_{fg}} q_w'' \tag{1.13}$$

and the fraction of heater's area exposed to boiling is determined from [Podowski, 2010] as

$$A_b'' = \left(\frac{\Delta T_w - \Delta T_0}{\Delta T_{nucl} - \Delta T_0} \right)^2 \tag{1.14}$$

where ΔT_w is the wall superheat, ΔT_0 is the minimum wall superheat required for nucleation, and ΔT_{nucl} is the wall superheat in well-established (saturated) nucleate boiling.

The current model provides a consistent solution for the wall temperature throughout the subcooled region and into the saturated boiling region. Its form allows for the investigation of individual phenomena associated with vapor generation.

In addition to the direct vapor generation model, a separate model of vapor condensation on the wall is included in the overall model. "Standing" bubbles which are formed at high subcooling but condense before they are able to depart from the wall are accounted for by this model. This allows boiling heat transfer to begin cooling the wall while there is practically no net generation of vapor, as observed in several experiments [Bartolomei & Chanturia, 1967] [Rouhani, 1966]. The model assumes that the heat transfer to a single "standing" bubble can be modeled as

$$q_0 = A_b H_{w,cond} \Delta T_l \tag{1.15}$$

where the wall-condensation heat transfer coefficient is calculated from Eq. (1.), with the\ necessary adjustments associated with the neat-wall conditions. For example, the Reynolds number for a bubble on the wall is determined assuming the vapor phase has zero velocity, i.e. bubbles are attached to the wall

$$\mathrm{Re}_{b,w} = \frac{\rho_l \left| \bar{u}_l \right| D_b}{\mu_l} \tag{1.16}$$

The wall condensation rate is be characterized by the condensation number, which represents the ratio of the heat transfer due to condensation to the maximum achievable heat transfer from condensation of all available vapor [Shaver et al., 2013]

$$Co = \frac{6 H_{w,cond} \left(T_{sat} - T_l \right)}{D_b \rho_v f h_{fg}} \leq 1 \tag{1.17}$$

where f is the ebullition frequency. The wall condensation rate is then given by

$$\Gamma_{w,v-l} = Co \Gamma_{w,l-v} \tag{1.18}$$

By formulating the condensation model in this manner, the nucleation site density is implicitly determined from the boiling rate, rather than from a correlation. This provides a physically consistent formulation.

1.4. Modeling of condensation-driven bubble collapse in subcooled boiling

The proposed model is based on the principle of counting and tracking the number of bubbles produced and transported throughout the flow domain. By combining the conservation of mass for a single moving bubble in the Lagrangian frame of reference with the vapor phase conservation of mass equation in the stationary Eulerian frame of reference, the following transport equation for bubble number density has been obtained [Shaver and Podowski, 2013a]

$$\frac{\partial n'''}{\partial t} + \nabla \cdot \left(\vec{u}_v n''' \right) = 0 \tag{1.19}$$

where the position- and time- (for transients) dependent bubble diameter is given by

$$V_b = \frac{\alpha}{n'''} \tag{1.20}$$

and α is the local void fraction.
In the case of subcooled boiling in heated pipes or reactor coolant channels, a non-zero boundary condition must be used on the heated wall, given by

$$\left(\vec{u}_v n''' \right)_{wall} = \frac{\Gamma''_{w,l-v}}{\rho_v V_{b,0}} \vec{e}_w \tag{1.21}$$

where $\Gamma''_{w,l-v}$ is the net vapor generation rate per unit wall area, $V_{b,0}$ is the average volume of bubbles departing the wall and $\vec{e}_w$ is the wall normal unit vector.
The contour plots of the: bubble diameter distribution, vapor volume fraction, interfacial condensation rate, and liquid subcooling are shown in Figure 1.1.
The new model has been compared against the existing constant bubble-diameter model. The results are shown in Fig. 1.2.

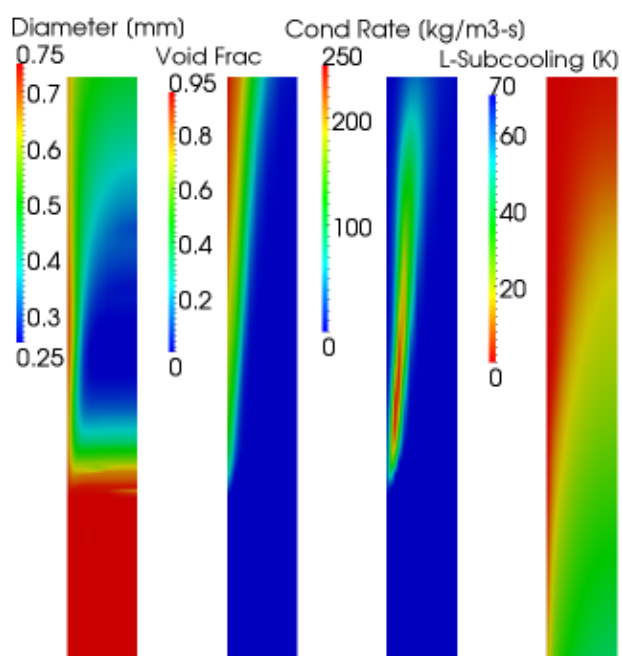

Fig. 1.1. Contour plots of bubble diameter, vapor volume fraction, interfacial condensation rate, and liquid subcooling for the last two thirds of the channel [Shaver et al., 2013a].

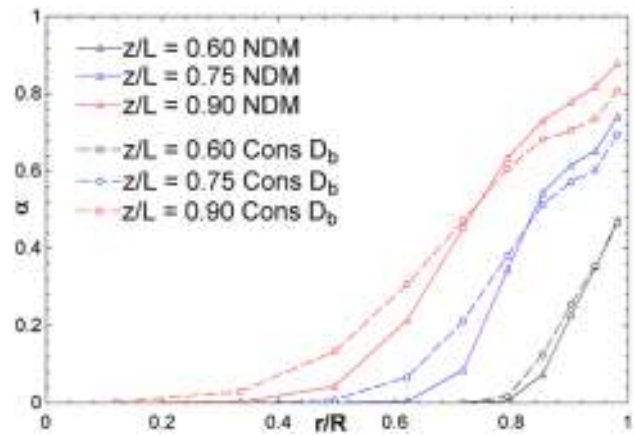

Figure 1.2. Radial profiles of the vapor volume fraction and interfacial condensation rate [Shaver et al., 2013a].

In general, the constant-bubble-size model may overpredict the near-wall condensation rate and at the same time shows a slower and more gradual decrease in bubble concentration toward the center of the pipe. If the condensation-induced bubble shrinking is accounted for, the near-wall void fraction is higher, but so is the condensation rate when the decreasing-size bubbles move away from the wall. This, in turn, may significantly increase the area of the single-phase liquid region in the central part of the pipe and the liquid subcooling there.

1.5. Advanced mechanistic model of near-wall heat transfer in subcooled boiling

A consistent mechanistic model of subcooled boiling heat transfer has been formulated based on the analysis of bubble ebullition cycle [Podowski & Shaver, 2013]

Using separate models for bubble diameter and nucleation frequency, the wall superheat can be determined from a newly developed model based on averaging time-dependent temperature oscillations during the ebullition cycle [Podowski and Shaver, 2013]. Specifically, using the heated wall energy conservation equations for dwell and growth periods, respectively

$$\rho_s c_{p,s} \delta_s \frac{d(\Delta T_w)}{dt} = q''_H - q''_{D,i} \tag{1.22}$$

$$\rho_s c_{p,s} \delta_s \frac{d(\Delta T_w)}{dt} = q''_H - q''^{evap}_{G,i} A''_b - q''^{l}_{G,i}(1 - A''_b) \tag{1.23}$$

yields the following relationship between the average wall temperature, wall heat flux and total bubble departure time

$$\frac{\sqrt{\pi}}{2\beta_l}\left(1 - \frac{A''_b}{\eta^3}\right)\frac{q''_H}{\Delta T_w^{satb}}\tau_{tot} - \sqrt{\tau_{tot}}(1 - A''_b) = \frac{2\beta_l}{\sqrt{\pi}}\frac{\Delta T_w^{satb}}{q''_H}A''_b \tag{1.24}$$

In Eqs.(1.22)-(1.24), q''_H is the heating rate per unit wall surface area, $q''^{evap}_{G,i}$ is the evaporation component of the surface heat flux during bubble growth, $q''^{l}_{G,i}$ and $q''_{D,i}$ are the single-phase heat fluxes during the growth and dwell periods, respectively, A''_b is the bubble surface density during the growth period, $\eta = (V_{b,o}/V_{b,d})^{1/3}$, $V_{b,d}$ and $V_{b,o}$ are the bubble volume at departure and the

equilibrium bubble volume, respectively, $\beta_l = k_l / \sqrt{\alpha_l}$, and the remaining notation is conventional.

1.6. Numerical Implementation

This model has been implemented in the state-of-the-art NPHASE-CMFD computer code [Antal, 2011], which independently solves conservation of mass, momentum and energy equations for any given number of fluid components (fields), along with turbulent quantities (k and ε) for the continuous field. The conservation of energy equation used for each fluid component in the NPHASE-CMFD code is given by [Antal, 2011]

$$\frac{\partial}{\partial t}\left(\alpha_j \rho_j h_j\right) + \nabla \cdot \left(\alpha_j \rho_j \bar{u}_j h_j\right) = \nabla \cdot \left[\alpha_j \left(\bar{q}''_j + \bar{q}''_{j,turb}\right)\right] + \sum_{i \neq j}^{I} \left(\Gamma_{i-j} h_i - \Gamma_{j-i} h_j\right) + S'''_j \tag{1.25}$$

where the subscripts i and j indicate the individual fluid component fields and S'''_j represents a general source term that can be used to model interfacial heat transfer. Note that certain terms are negligible and are not included in the present formulation (e.g. viscous dissipation).

1.6.1. Interfacial Heat and Mass Transfer

The proposed interfacial heat and mass transfer model is capable of accounting for both subcooled liquid and superheated vapor. In order to model interfacial condensation, the desired form of the energy equations for the liquid and vapor fields respectively is given by [Shaver et al., 2013a]

$$\frac{\partial}{\partial t}\left(\alpha_l \rho_l h_l\right) + \nabla \cdot \left(\alpha_l \rho_l \bar{u}_l h_l\right) = \nabla \cdot \left[\alpha_l \left(\bar{q}''_l + \bar{q}''_{l,turb}\right)\right] + \Gamma_{v-l} h_f + q'''_l \tag{1.26}$$

$$\frac{\partial}{\partial t}\left(\alpha_v \rho_v h_v\right) + \nabla \cdot \left(\alpha_v \rho_v \bar{u}_v h_v\right) = -\Gamma_{v-l} h_g + q'''_v \tag{1.27}$$

On the other hand, the NPHASE-CMFD formulation is

$$\frac{\partial}{\partial t}\left(\alpha_l \rho_l h_l\right) + \nabla \cdot \left(\alpha_l \rho_l \bar{u}_l h_l\right) = \nabla \cdot \left[\alpha_l \left(\bar{q}''_l + \bar{q}''_{l,turb}\right)\right] + \Gamma_{v-l} h_v + S'''_l \tag{1.28}$$

$$\frac{\partial}{\partial t}\left(\alpha_v \rho_v h_v\right) + \nabla \cdot \left(\alpha_v \rho_v \bar{u}_v h_v\right) = -\Gamma_{v-l} h_v + S'''_v \tag{1.29}$$

Note that the diffusion term is not included in the vapor energy equation, since direct heat transfer does not occur between dispersed bubbles. Two energy source terms are used for each fluid component, one representing the energy associated with adding or removing mass from a field and the other representing sensible heat transfer. The default behavior is to have the source term associated with mass transfer carry the enthalpy of the donor field. Therefore, the source term in NPHASE-CMFD must be adjusted to ensure that mass is generated or removed at the proper enthalpy. Specifically, we write

$$S'''_l = \Gamma_{v-l}\left(h_f - h_v\right) + q'''_l \tag{1.30}$$

$$S'''_v = \Gamma_{v-l}\left(h_v - h_g\right) + q'''_v \tag{1.31}$$

The gamma terms in these two equations can then be interpreted as a correction for superheated vapor. For the case of saturated vapor, it can be shown that the volumetric heat sources in the energy equations become

$$q_l''' = \Gamma_{v-l} h_{fg} \tag{1.32}$$

$$q_v''' = 0 \tag{1.33}$$

and the source terms used in the NPHASE-CMFD formulation convert to

$$S_l''' = \Gamma_{v-l}\left(h_g - h_v\right) \tag{1.34}$$

$$S_v''' = \Gamma_{v-l}\left(h_v - h_g\right) \tag{1.35}$$

Then, the NPHASE-CMFD form of the energy conservation equations becomes

$$\frac{\partial}{\partial t}\left(\alpha_l \rho_l h_l\right) + \nabla \cdot \left(\alpha_l \rho_l \vec{u}_l h_l\right) = \nabla \cdot \left[\alpha_l \left(\vec{q}_l'' + \vec{q}_{l,turb}''\right)\right] + \Gamma_{v-l} h_g \tag{1.36}$$

$$\frac{\partial}{\partial t}\left(\alpha_v \rho_v h_v\right) + \nabla \cdot \left(\alpha_v \rho_v \vec{u}_v h_v\right) = -\Gamma_{v-l} h_g \tag{1.37}$$

which is consistent with the corresponding theoretical formulation.

1.6.2. Vapor Generation

The treatment of the vapor generation models is much more straightforward since the quenching heat transfer (i.e. the heat required to increase the liquid enthalpy to saturation) can be handled explicitly as {Shaver et al., 2013a]

$$\Gamma_{l-v,w} h_{lg} = q_b''' \tag{1.38}$$

where h_{lg} represents the enthalpy difference between the local (possibly subcooled) liquid and saturated vapor. The desired forms of the energy equations are then given by

$$\frac{\partial}{\partial t}\left(\alpha_l \rho_l h_l\right) + \nabla \cdot \left(\alpha_l \rho_l \vec{u}_l h_l\right) = \nabla \cdot \left[\alpha_l \left(\vec{q}_l'' + \vec{q}_{l,turb}''\right)\right] - \Gamma_{l-v,w} h_l + \Gamma_{v-l,w} h_v + q_{1\phi}''' \tag{1.39}$$

$$\frac{\partial}{\partial t}\left(\alpha_v \rho_v h_v\right) + \nabla \cdot \left(\alpha_v \rho_v \vec{u}_v h_v\right) = \Gamma_{l-v,w} h_l - \Gamma_{v-l,w} h_v + q_b''' \tag{1.40}$$

Note that the volumetric single phase and boiling heat transfer terms must be properly translated using the local wall area and nodal volume. It is apparent that no correction terms are required for this model and the source terms in NPHASE-CMFD become

$$S_l''' = q_{1\phi}''' = q_{1\phi}'' \frac{A_w^{cell}}{V_w^{cell}} \tag{1.41}$$

$$S_v''' = q_b''' = q_b'' \frac{A_w^{cell}}{V_w^{cell}} \tag{1.42}$$

Since vapor generation determined in this manner is purely a wall effect, the associated terms in the energy equations are only active in the near-wall nodes, whereas the interfacial heat and mass transfer terms are active throughout the domain.

It is well known that liquid temperature experiences a steep drop in the near-wall region. In order to address this issue and to assure the independence of the calculated condensation rate of the computational mesh size, the reference liquid temperature, T_l, in Eq.(1.16) has been evaluated at a distance from the wall equal to ¾ of bubble diameter. This provides a realistic average temperature the bubble surface is exposed to, while assuming that not all bubbles are fully grown when they begin condensing.

1.7. Validation of new models against experimental data

A multiple step approach has been used to test and validate the new models of two-phase flow and subcooled boiling heat transfer.

The first step was to perform extensive parametric studies on the consistency of the proposed models of interfacial phenomena. An example illustrating the sensitivity effect of varying a single modeling parameter is shown in Figure 1.3 [Jiao and Podowski, 2012].

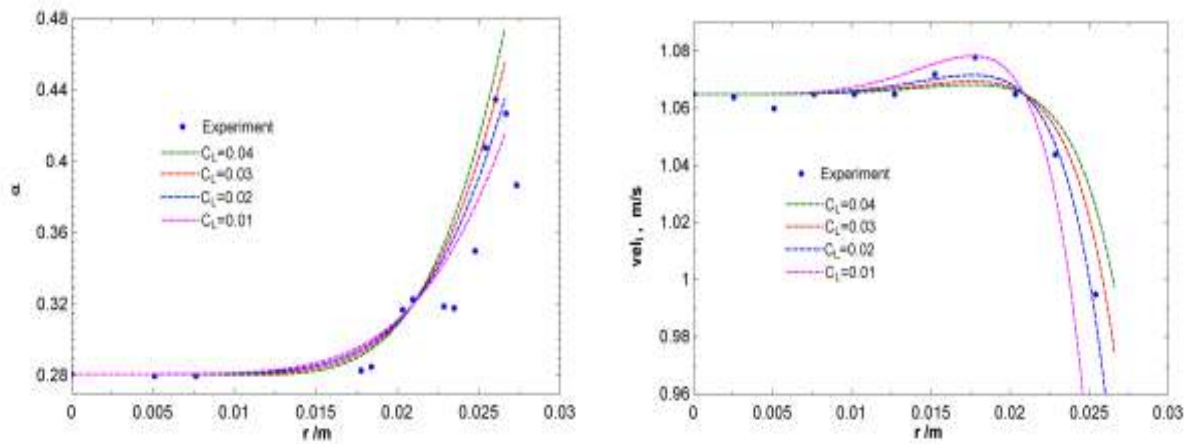

Figure 1.3. Parametric testing of RPI two-phase flow model against the experimental conditions of Wang et al. for air/water flow [Jiao and Podowski, 2012].

The next step was to perform a thorough validation of the overall two-phase flow model. Typical results for a series of experimental conditions used by Wang et al. are shown in Figure 1.4.

Finally, the validation of subcooled boiling models was performed using tow experimental data sets as a reference. A comparison between the calculations and the results of experiments performed by Bartolomei and Chanturia [1967] are shown in Figure 1.5 [Shaver et al., 2013a]. Similar results for the experiments performed by Rouhani [1966] for a flow inside an annulus with a heated central rod are shown in Figure 1.6. A comprehensive analysis of the model's predictions, including the two above mentioned experiment as well as an additional data set, is currently underway.

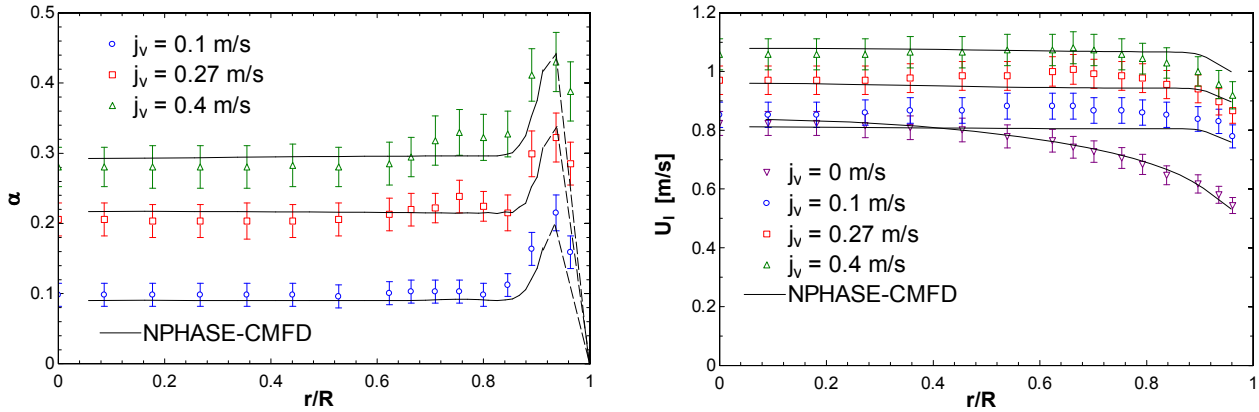

Figure 1.4. Validation of the RPI two-phase flow model against experimental data for air/water flow [Shaver et al, 2012].

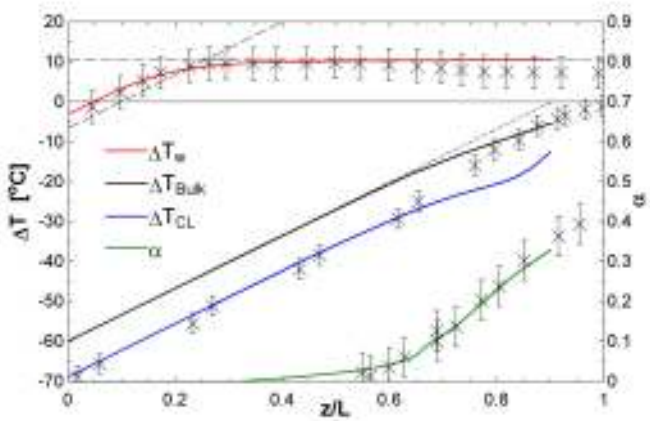

Figure 1.5. The calculated bulk liquid temperature, wall superheat, and radially-averaged volume fraction of vapor, compared to experimental data of Bartolomei and Chanturia [1967]. The dashed lines correspond to the wall temperature predicted using the Dittus-Boelter correlation (for single-phase flow) and the Jens-Lottes correlation (for boiling conditions).

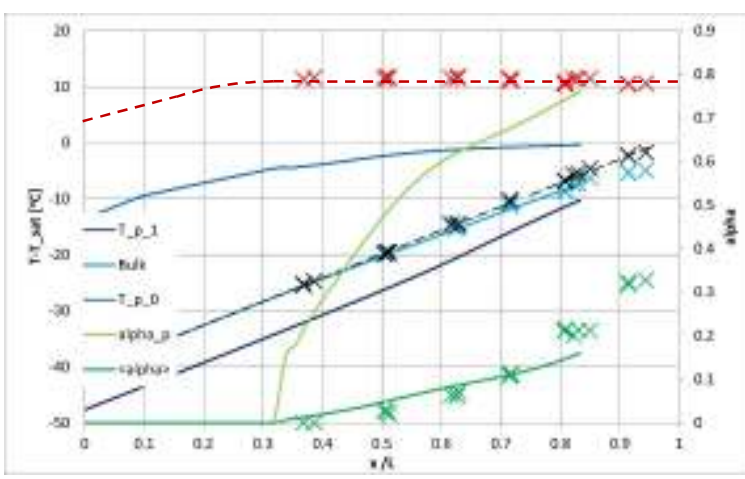

Figure 1.6. The calculated bulk liquid temperature, wall superheat, and radially-averaged volume fraction of vapor, compared to experimental data of Rouhani [1966].

1.8. Model application to actual geometry of PWR coolant channels

Test calculations have been carried out for a PWR coolant channel surrounded by four sections of uniformly heated fuel elements [Podowski & Shaver, 2013].

The predicted local coolant temperature and void fraction distributions are shown in Figure 1.7. As can be seen, a highly subcooled liquid at channel inlet gets gradually heated along the flow, to reach the saturation temperature close to channel exit. At the same time, since the cladding wall temperature exceeds saturation at about two-thirds along the flow, local near-wall boiling occurs along the upper sections of the fuel pins. As can be seen, the void distribution at channel exit is highly nonuniform, reaching a near-wall peak value of over 30% while still remaining very low at channel center.

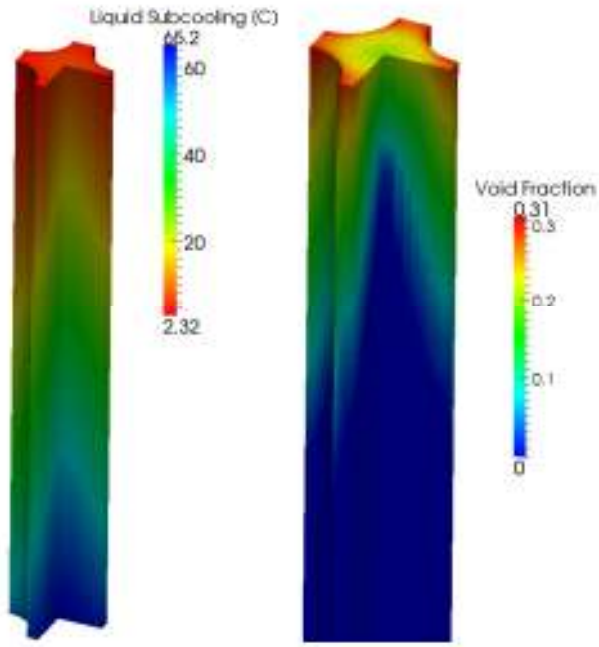

Figure 1.7. Local liquid subcooling and void fraction distributions in a reactor coolant channel.

Detailed Report for Sub-Milestone 2

2.1. Modeling formulation

The Level-set-based method applied to systems with phase change is based on the following equations:

Level-set advection equation

$$\frac{\partial \phi}{\partial t} + \nabla \cdot (\bar{u}\phi) = \frac{\Gamma``}{\rho_l} \tag{2.1}$$

Level-set re-initialization equation

$$\frac{\partial \phi}{\partial \tau} = S(\phi_0)(1 - |\nabla \phi|) \tag{2.2}$$

To assure that the level-set function is properly defined as a signed distance function to the interface, the solution of Eq.(2.2) must satisfy the following condition

$$|\nabla \phi| = 1 \tag{2.3}$$

The model of moving vapor bubbles with phase change due to evaporation and/or condensation is given by

Continuity Equation

$$\nabla \cdot u = \Gamma''(\frac{1}{\rho_v} - \frac{1}{\rho_l})\frac{A_{evap}}{V} \tag{2.4}$$

where the corresponding evaporation rate term is

$$\Gamma'' = \frac{k}{c_p}\frac{h - h_f}{\phi}\frac{1}{h_{fg}} \tag{2.5}$$

Bubble/liquid interface curvature equation

$$\kappa(\phi) = \nabla \cdot (\frac{\nabla \phi}{|\nabla \phi|}) \tag{2.6}$$

Energy conservation energy equation

$$\frac{\partial h}{\partial t} + \nabla \cdot (hu) = \frac{k \nabla^2 h}{\rho(\phi) c_p} \tag{2.7}$$

Eqs.(2.1)-(2.7) have been incorporated in the NPHASE-CMFD code and coupled with the other governing equations within this code.

2.2. Parametric model testing

The new model has been parametrically tested for several flow and heat transfer conditions, including both 2-D and 3-D simulations.

Figure 2.1 shows the motion of a small (about 1 mm diameter) 2-D steam bubble surrounded by quiescent superheated liquid water. The pressure is 101 kPa and the liquid superheat is 10oC.

The results of a full 3-D simulation for similar conditions are shown in Figure 2.2, and the corresponding velocity vectors are shown in Figure 2.3.

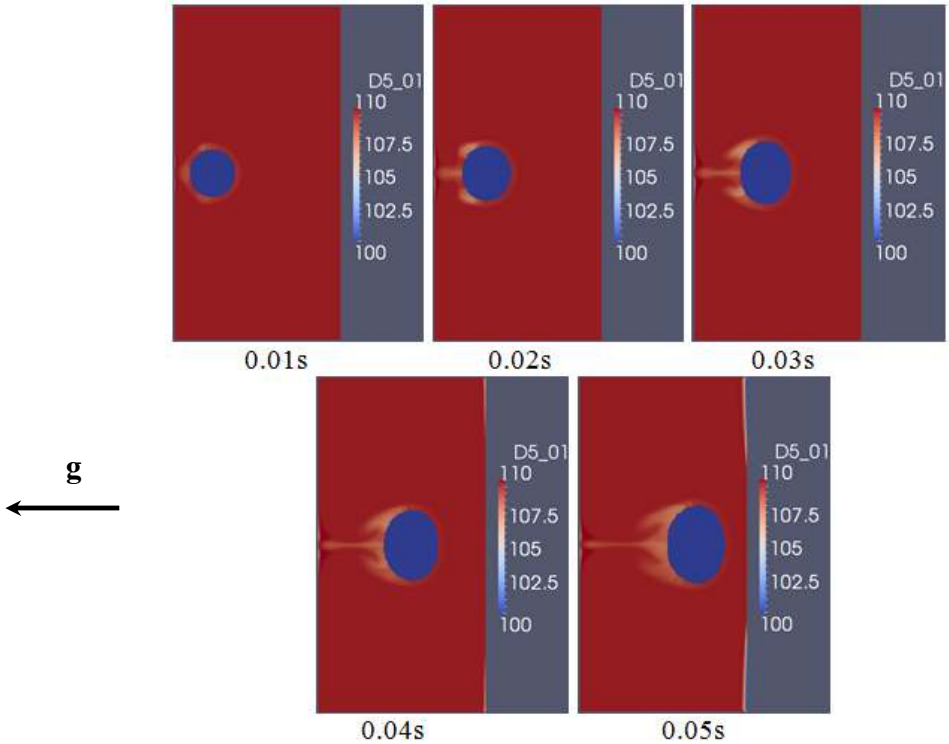

Figure 2.1. Temperature profiles at different time instants for a gravity-driven motion of 2-D vapor bubble surrounded by superheated liquid [Jiao and Podowski, 2013a].

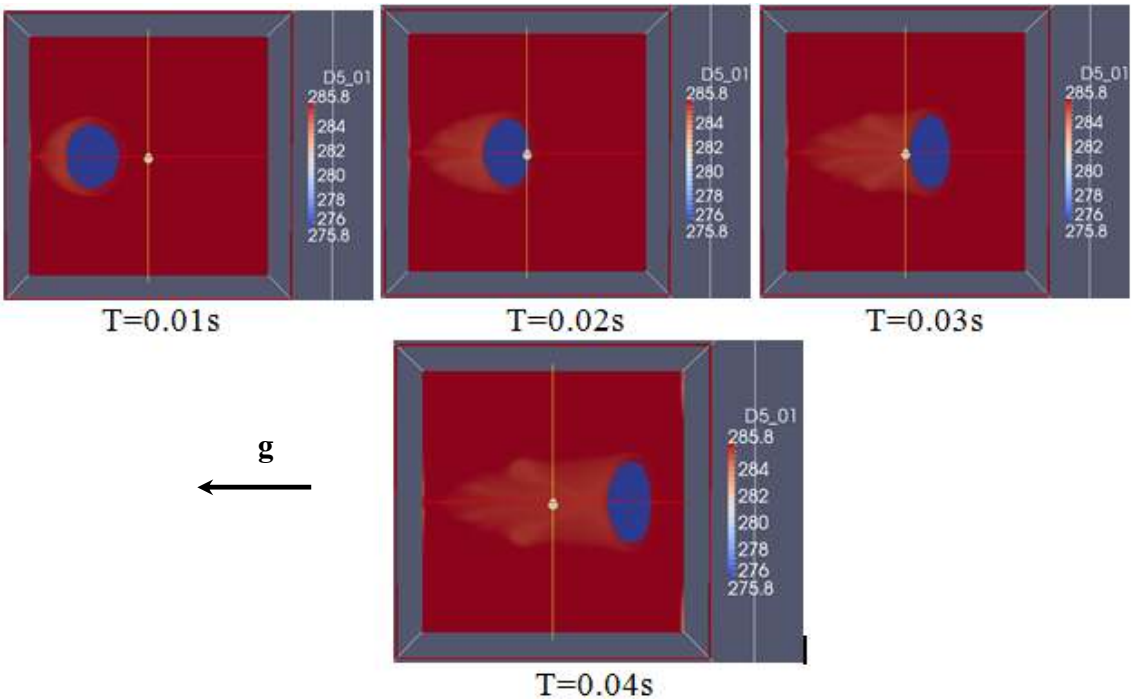

Figure 2.2. Temperature profiles at different time of a gravity-driven motion of 3-D vapor bubble surrounded by superheated liquid [Jiao and Podowski, 2013a].

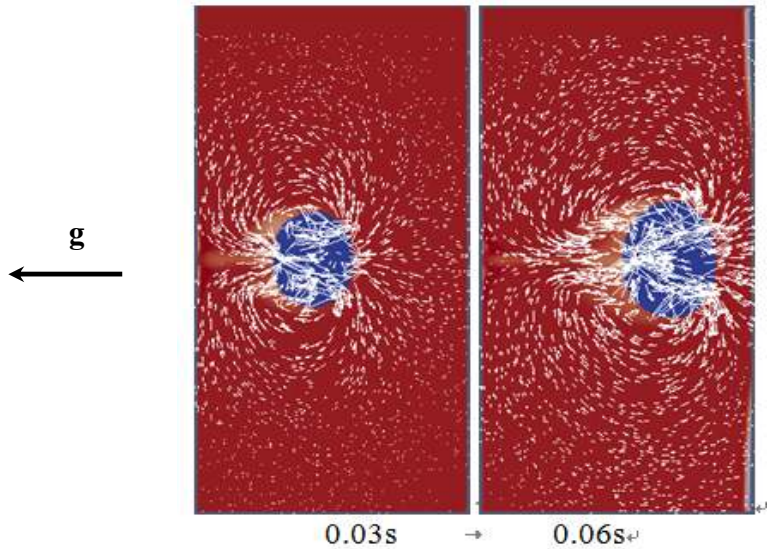

Figure 2.3. Velocity vectors around a growing moving bubble [Jiao and Podowski, 2013a].

A similar series of simulations has been also performed for a gravity-driven steam bubble surrounded by subcooled liquid water at 90°C. As can be seen in Figure 2.4, he bubble gradually shrinks due to condensation, leaving a trail of warmer liquid.

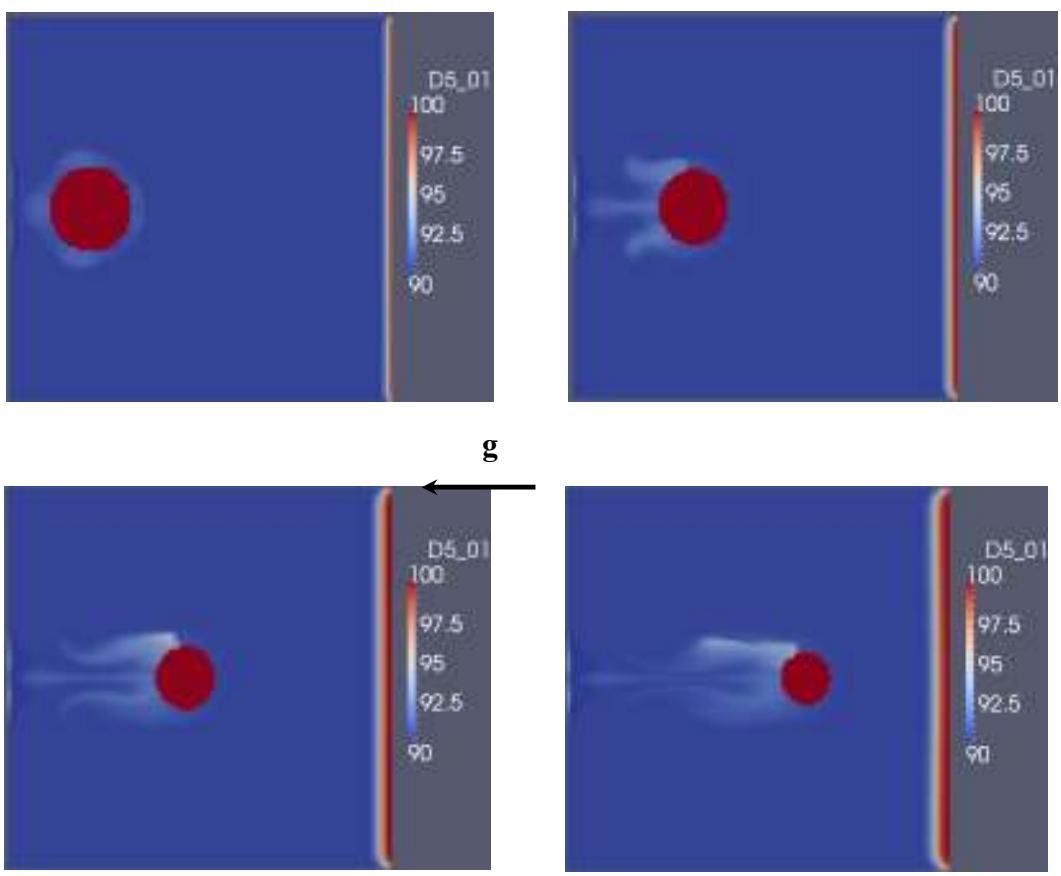

Figure 2.4. Temperature profiles at different time of a gravity-driven motion of 2-D vapor bubble surrounded by subcooled quiescent liquid [Jiao and Podowski, 2013b].

A generalization of the results shown in Figures 2.1 and 2.4 is presented in Figures 2.5 and 2.6. In this case, a prescribed liquid temperature gradient is applied along the bubble motion, from a 10ºC superheat to a 10ºC subcooling. As can be noticed in Figure 2.5, the bubble first grows slightly due to evaporation in contact with superheated water, then when moving against gravity, its tip gets exposed to subcooled liquid which triggers local condensation. The fractions of bubble surface which are subject to either evaporation of condensation are clearly seen in Figure 2.6.

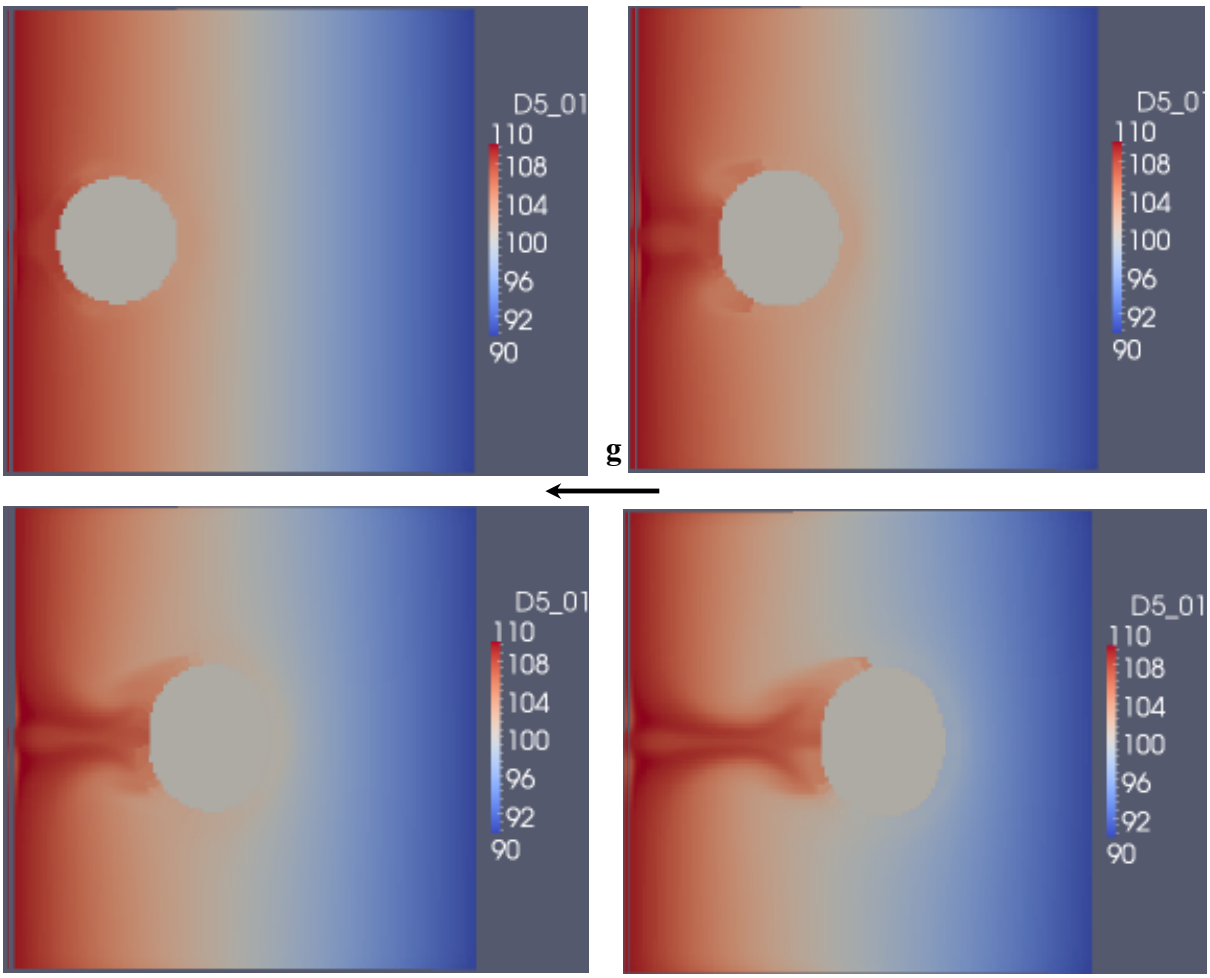

Figure 2.5. Temperature profiles and bubble shape during a gravity-driven motion from along a variable-temperature liquid field. The snapshots correspond to: 0.01s and 0.02s (upper parts) and 0.03s and 0.04s (lower parts). The bubble is subject first to evaporation (the upper figures) and then to simultaneous evaporation and condensation (the lower figures) [Jiao and Podowski, 2013b].

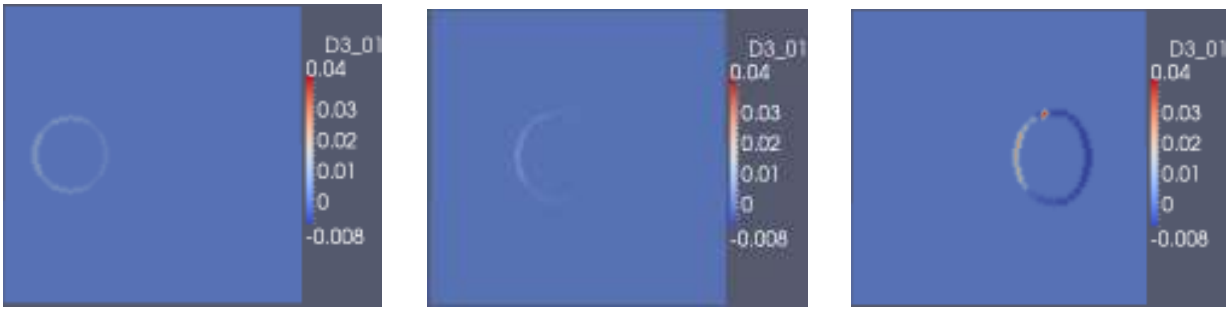

Figure 2.6. Phase change rates for the bubble in Figure 2.5 [Jiao and Podowski, 2013b].

The current model has also been applied to flow boiling conditions. Specifically, bubble motion was simulated in shear flow near a heated wall subject to a steep temperatrue gradient. The simulations have been performed at a prototipical reactor pressure of 16 MPa, which corresponds to a saturation temperature of 347.4oC. The results are shown in Figure 2.7.
The analysis of bubble trajectory illustrated in Fig. 2.7 has already resulted in important observations which will directly guide further improvements of the RANS-level model of subcooled boiling discussed in the summary of fork for Milestone-1. One of them is the fact that small bubbles tend to flow along the heated wall, which in turn leads to the buildup of vapor and an increase in the local void fraction there. The observation concerning sliding bubbles is apparently consistent with the recent experimental observations at MIT. Future simulations with multiple bubbles will be directly used to improve the accuracy of void distribution using the RANS model of two-phase flow.

2.3. Verification of numerical consistency and accuracy

To test the numerical convergence of the simulations, as well as the accuracy-control method used by the combined NPHASE/Level-Set model, test calculations have been performed for a buoyancy-drive motion of a steam bubble in a superheated liquid at a uniform (initially) temperature of 5°C above the saturation temperature. To demonstrate the performance of the model at a high liquid-to-vapor density ratio, the physical conditions corresponded to the atmospheric pressure. The calculations have been performed using three parallel processors for a two-dimensional domain discretized into 195 x195 nodes. The snapshot results of bubble-shape and temperature evolutions are shown in Figure 2.7. As can be seen, the initially circular bubble shape was gradually both growing and flattening, both effects as expected. The growth rate corresponded to the liquid-side heat flux and the flattening was due to the surface force imbalance across the bubble thickness between the inner vapor layer and the corresponding outer liquid layer. The liquid-to-bubble heat transfer rate is reflected in the liquid temperature gradient around the bubble surface. Since there is no net liquid flow along the domain, the cooled liquid left behind the bubble formed symmetrically distributed growing wakes.

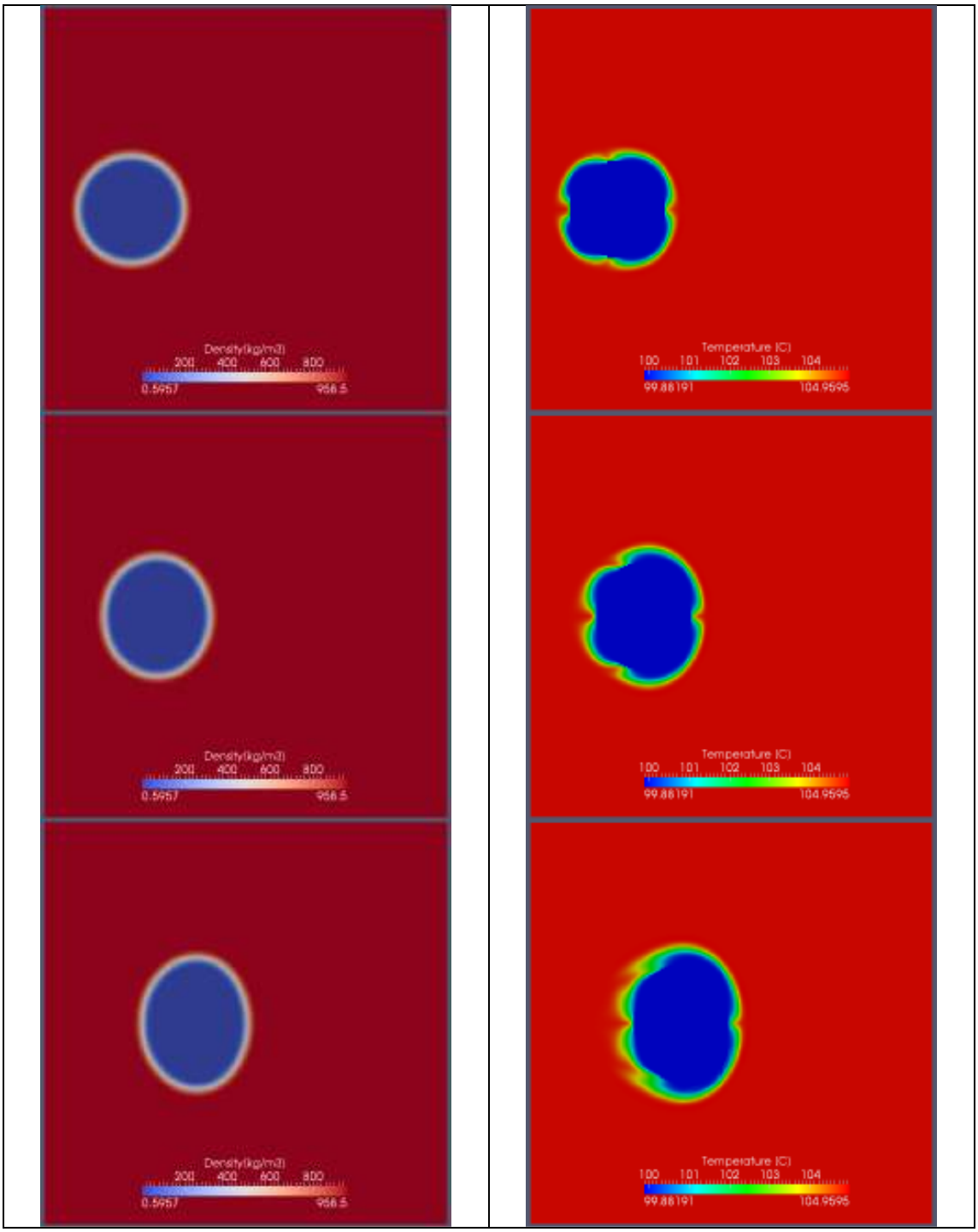

Figure 2.7(a). Bubble shape (indicated by vapor density) and liquid temperature field around a growing bubble moving due to buoyancy inside a volume of quiescent superheated liquid. The acceleration of gravity vector is directed from the right to the left. The snapshots correspond to 0.01 s time/ intervals, starting at 0.01 s.

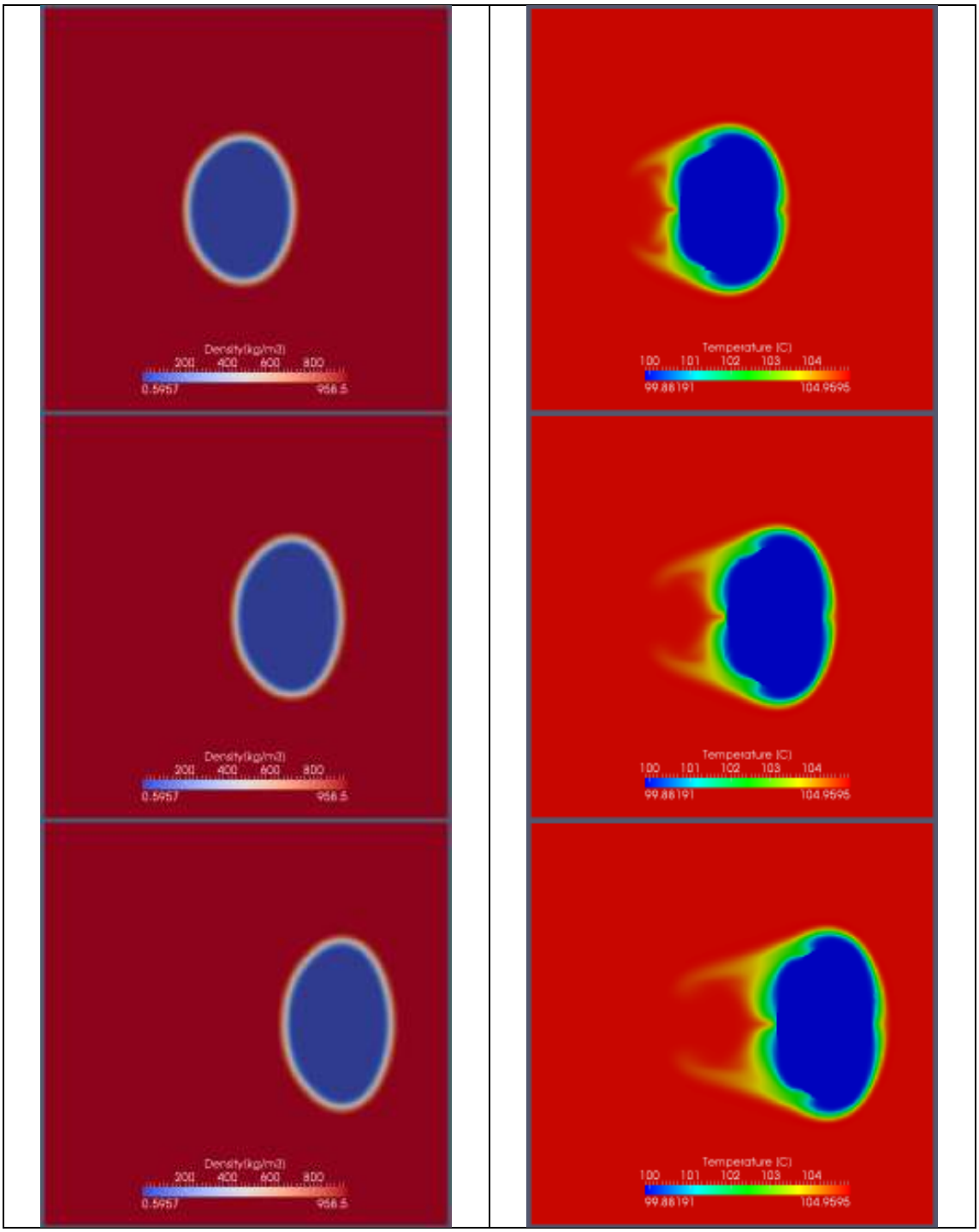

Figure 2.7(a). Continuation of Figure 2.7(a); the snapshots correspond to 0.4 s, 0.05 s and 0.06s.

The preservation of the conservation of mass and energy principles has been checked by comparing the heat-transfer-drive mass of the bubble between the final and the initial states using two different methods. In one of them, the bubble mass change based on the integrated phase change rate in the interfacial region. In the other approach, the differential mass change has been calculated by summing up

the volume of all cells containing vapor at each the final and initial stare. A comparison between the results for both methods are shown in Table 2.1. As can be seen, a very good agreement between the two methods has been obtained.

Table 2.1. Confirmatory results for mass conservation due to phase change

Initial bubble mass [kg]	Final bubble mass [kg]	Fractional mass increase, relative to initial mass	Mass change based on integrated phase change rate [kg]	Mass change based on bubble volume increase between the initial and final time steps [kg])
1.88E-09	3.34E-09	7.77E-01	1.46E-09	1.45E-09

The results shown in Figure 2.7 have also been used to evaluate the velocity of the accelerating bubble. Both the trend of velocity change and the magnitude of the bubble velocity are consistent with both experimental observations and the predictions by one-dimensional model.

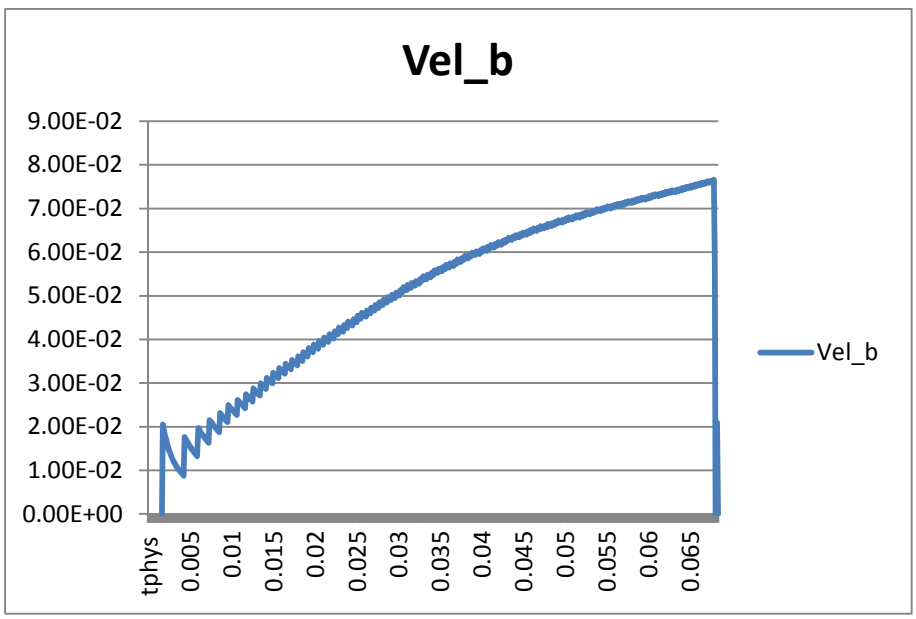

Figure 2.8. Velocity of buoyancy-driven accelerating bubble.

2.4. Model application to simulated subcooled boiling conditions

Another outcome of the simulations shown in Figure 2.7 deals with a first-principle approach to predict bubble size evolution in subcooled boiling very close to heated wall. This part of the current RANS model of subcooled boiling is based on an assumed fixed bubble diameter. The results shown I n Fig. 2.7 can be considered as the first step toward formulating a fully mechanistic RANS model of simultaneous evaporation and condensation phenomena and the resultant bubble

size evolution as they gradually move away from the wall into the subcooled liquid region. The work to formulate such models is underway.

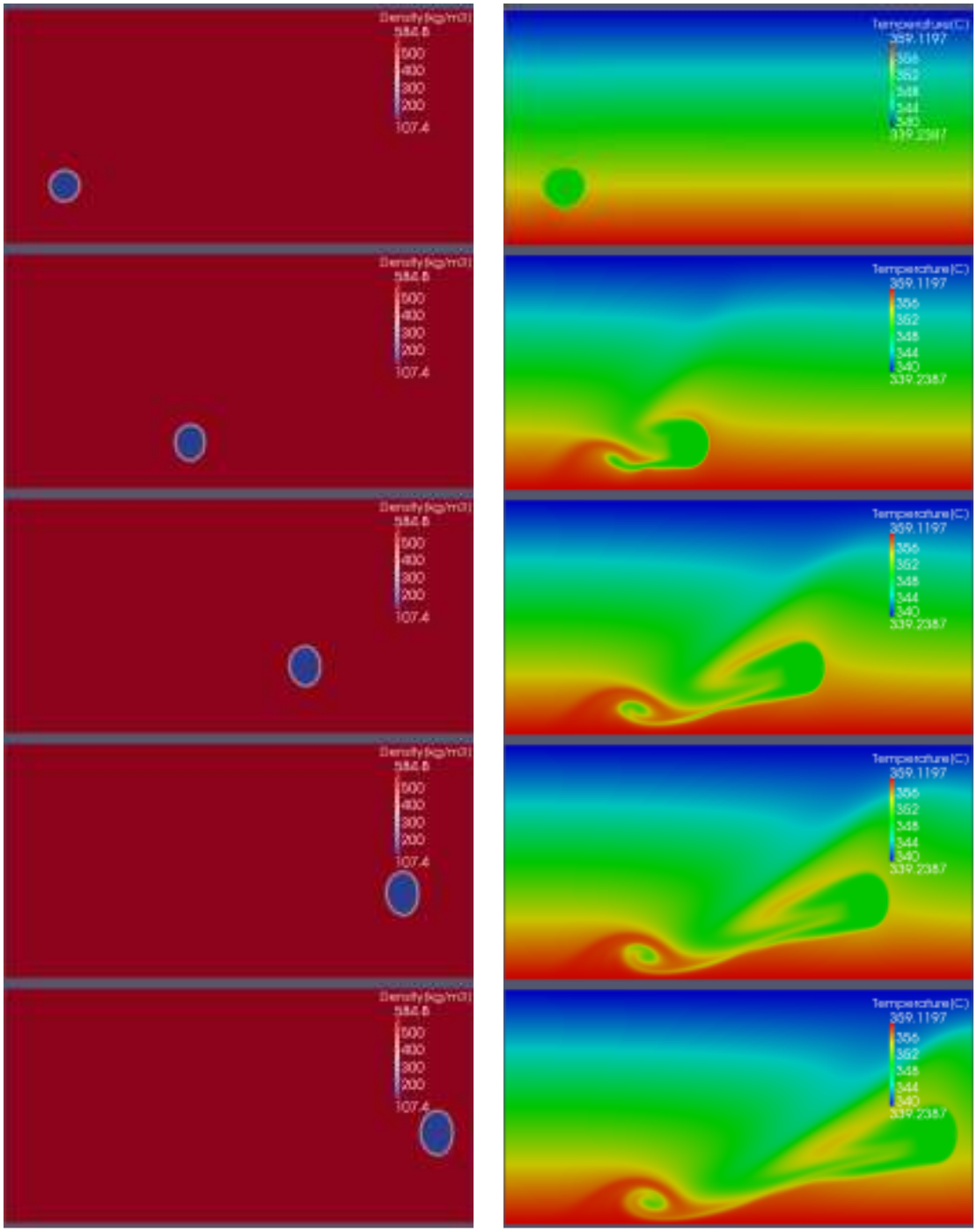

Figure 2.7. Simulation of bubble motion is shear flow near a heated wall in subcooled boiling at 16MPa [Jiao and Podowski, 2013b].

Critical Issues for the Development of an Advanced Mechanistic Model of Subcooled Boiling in PWR Fuel Assemblies

Several modeling and computational issues will still have to be resolved to develop and implement a PWR thermal-hydraulics model as part of the CASL virtual reactor. Two issues which are critical for the formulation of a complete accurate model of subcooled boiling in actual PWR fuel assemblies capable of capturing the local flow and heat transfer phenomena over a full range of conditions, from nuclear boiling to boiling transition and temperature excursion (DNB), are:

(1) Mechanistic model of three-dimensional two-phase flow and subcooled boiling around spacer grids.

(2) Mechanistic model of DNB (CHF at low quality boiling, including subcooled boiling).

As an illustration of the feasibility of both tasks, selected results of the earlier works are shown next.

First, the ability of a consistent two-phase flow model to capture void fraction and pressure drop distributions around spacer grids is demonstrated using as a reference the experimental fuel assembly of FRIGG Loop. The corresponding figures have been taken from the following paper:

- H. Anglart, O. Nylund, N. Kurul and M.Z. Podowski, "CFD Simulation of Flow and Phase Distribution in Fuel Assemblies with Spacers", Nuclear Engineering and Design, 177, 1997.

The results of CHF predictions for a series of experiments, which are shown next, have been reported in the following papers:

- A. Alajbegovic, N. Kurul, M.Z. Podowski, D.A. Drew and R.T. Lahey, Jr., "A New Mechanistic Model of Critical Heat Flux in Forced-Convection Subcooled Boiling", Proc. 8th International Topical Meeting on Nuclear Reactor Thermal Hydraulics (NURETH-8), V. 2, Kyoto, Japan, 1997.
- M.Z. Podowski, "On the Mechanistic Multidimensional Modeling of CHF in Forced-Convection Boiling", Proc. 34th National Heat Transfer Conference, Pittsburgh, PA, 2000.
- M.Z. Podowski and S.P. Antal, "CFD Predictions of Temperature Excursion (CHF) in Low-Quality Boiling in Heated Channels", Proc. Twelfth International Heat Transfer Conference, Grenoble, France, 2002.

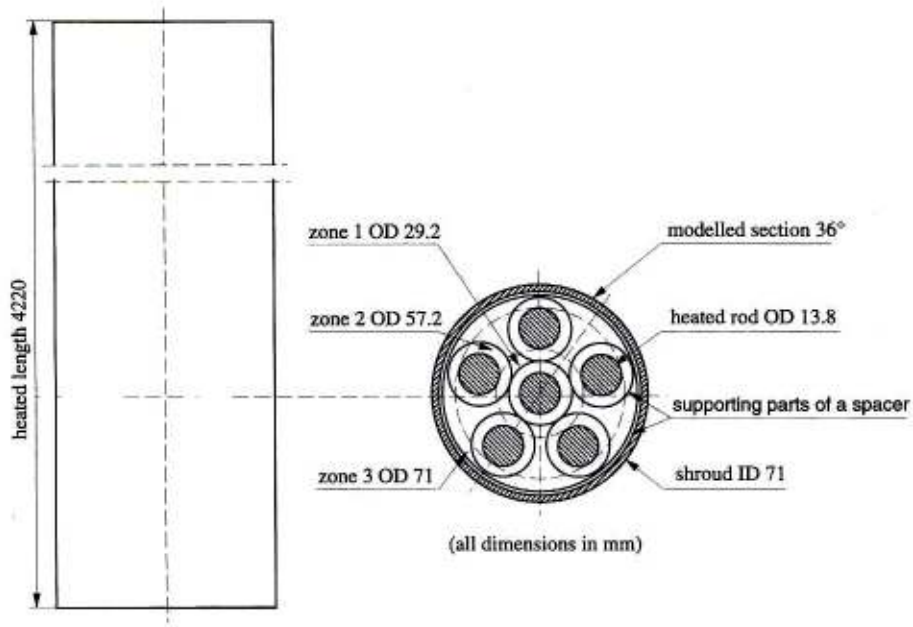

Fig. 1. Test section FT-6a of the early FRIGG Loop project.

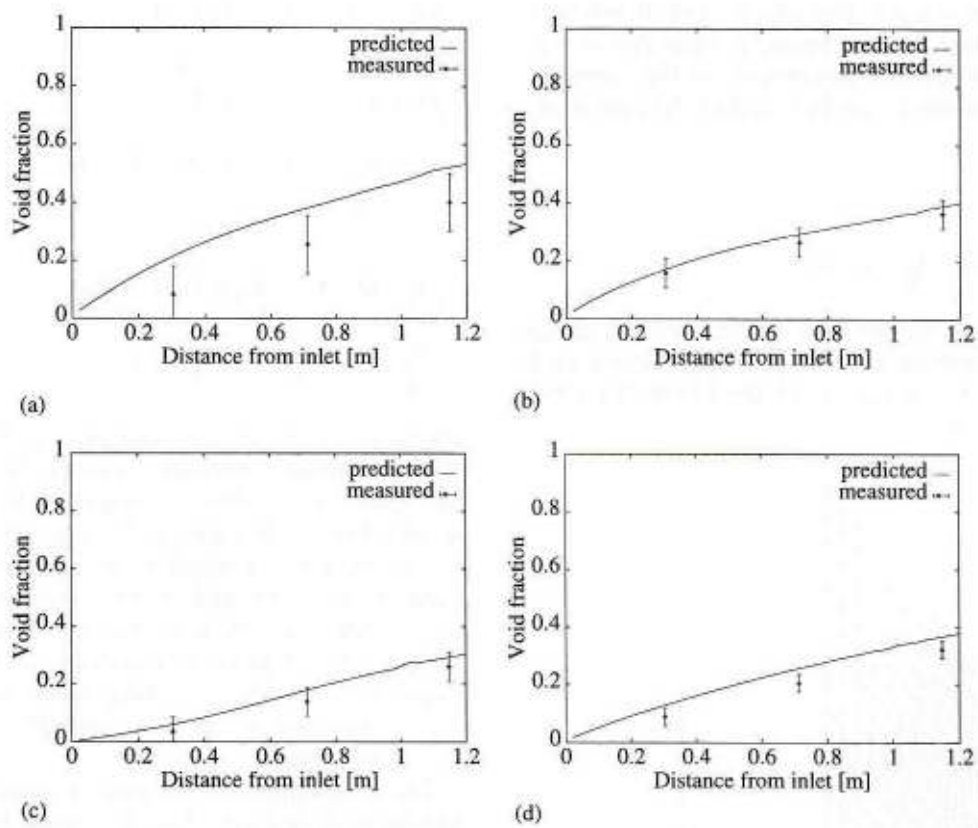

Fig. 3. Axial void distributions along the test section FT-6a; (a) zone 1; (b) zone 2; (c) zone 3; (d) mean in test section.

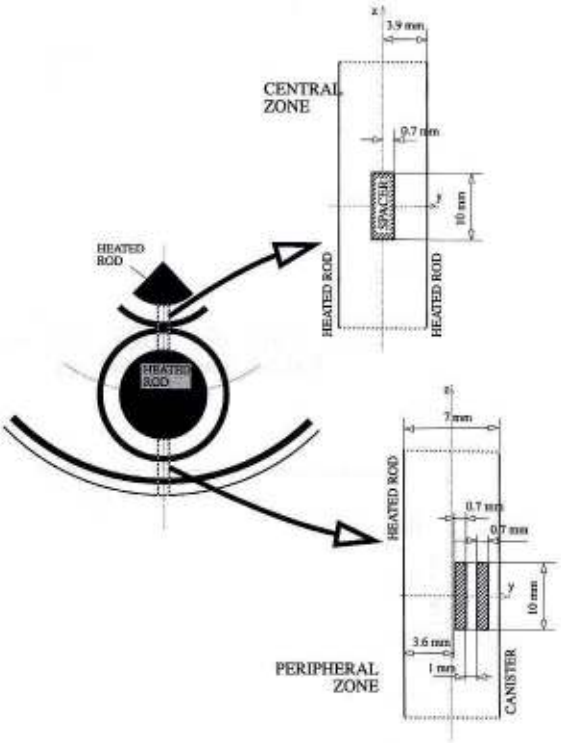

Fig. 6. The sections of the FT-6a assembly and corresponding computational geometry used in the present simulations.

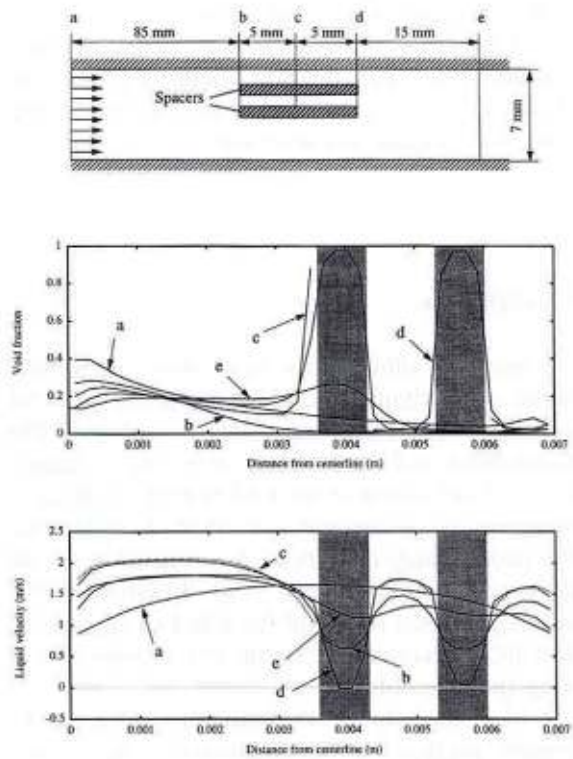

Fig. 14. The calculated void fraction distributions at several cross sections in the peripheral zone; inlet conditions obtained from 3-D calculations. $G = 1162$ kg m^{-2} s^{-1}, $a = 13\%$, (see Fig. 6 for the geometry).

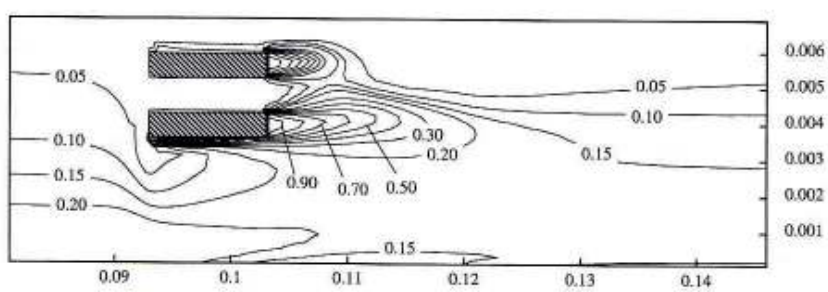

Fig. 13. The calculated constant void fraction lines in the peripheral zone; inlet conditions obtained from 3-D calculations. $G = 1162$ kg m^{-2} s^{-1}, $a = 13\%$ (see Fig. 6 for the geometry).

From: A. Alajbegovic, N. Kurul, M.Z. Podowski, D.A. Drew and R.T. Lahey, Jr., Proc. NURETH-8, V. 2, Kyoto, Japan, 1997.
M.Z. Podowski, Proc. 34th National Heat Transfer Conference, Pittsburgh, PA, 2000.
M.Z. Podowski and S.P. Antal, Proc. Twelfth International Heat Transfer Conference, Grenoble, France, 2002.

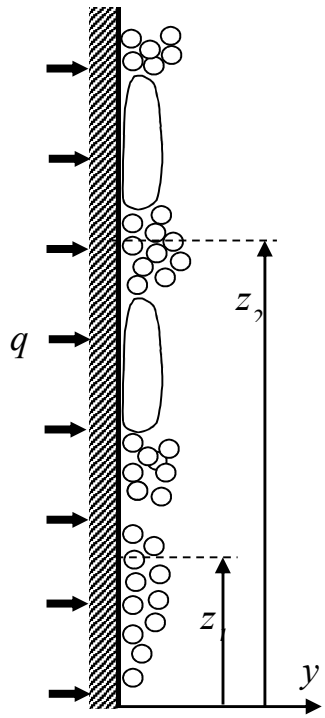

Formation of elongated bubbles in subcooled boiling prior to heated wall temperature excursion

Table 1: Predicted critical heat fluxes,

$G = 514\ kg/m^2s$

ΔT_{sub} [K]	Measured [6] $[kW/m^2]$	Predicted $[kW/m^2]$	Relative error
30	241	190	-21%
20	211	160	-25%
10	174	125	-28%

Table 2: Predicted critical heat fluxes,

$G = 1239 kg/m^2s$

ΔT_{sub} [K]	Measured [6] $[kW/m^2]$	Predicted $[kW/m^2]$	Relative error
30	332	405	+22%
20	277	302	+9%
10	244	170	-30%

[6] Hino, R. and Ueda, T., Studies on Heat Transfer and Flow Characteristics in Subcooled Flow Boiling-Part 2. Flow Characteristics," Int. J. Multiphase Flow, 11, 1985.

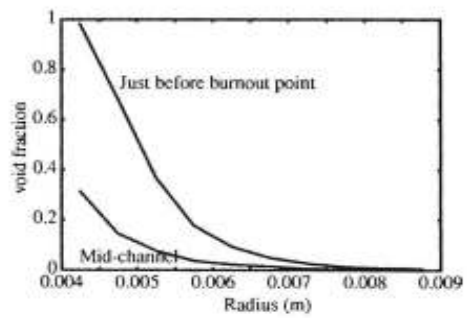

Axial Temperature Distributions obtained for the experimental data of Hino & Ueda [6], G=512 kg/s, ΔT_{in}= 30 °C, q"= 190 W/m^2, p= 0.147 MPa.

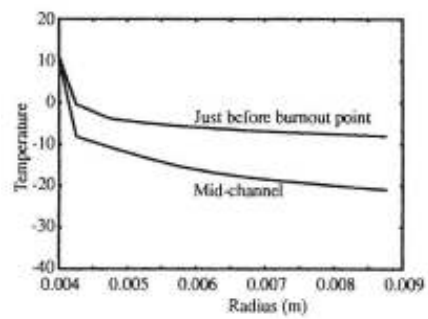

Radial temperature distribution obtained for the experimental data of Hino & Ueda [6], G=512 kg/s, ΔT_{in}= 30 °C, q"= 190 W/m^2, p= 0.147 MPa.

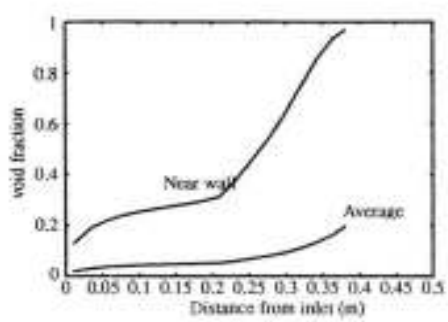

Axial void fraction distribution obtained for the experimental data of Hino & Ueda [6], G=512 kg/s, ΔT_{in}= 30 °C, q"= 190 W/m^2, p= 0.147 MPa.

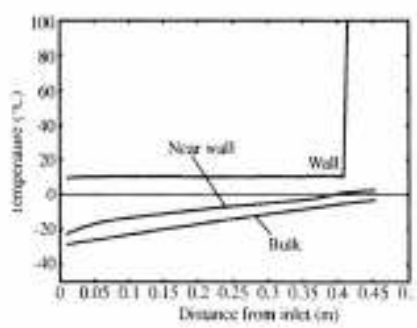

Axial Temperature Distributions obtained for the experimental data of Hino & Ueda [6], G=512 kg/s, ΔT_{in}= 30 °C, q"= 190 W/m^2, p= 0.147 MPa.

REFERENCES AND RECENT PROJECT-RELATED PUBLICATIONS

Note: Papers marked with (*) documet the results of research performed by the RPI Team for the CASL Project.

S.P. Antal (2011), "NPHASE-CMFD User Manual, Interphase Dynamics, LLC.

A. Bejan (2007), Convection Heat Transfer, John Wiley and Sons Inc., Hoboken, NJ.

D.A. Drew and R.T. Lahey, Jr. (1979), "Application of General Constitutive Principles to the Derivation of Multidimensional Two-Phase Flow Equations", Int. J Multiphase Flow, vol. 7, 243-264.

H. Jiao and M. Z. Podowski (2012), "An Analysis of Multidimensional Models of Gas/Liquid Flows", ANS Proc., 2012 Winter Meeting, San Diego, CA, pp.1393-1394.*

H. Jiao, S.P. Antal and M.Z. Podowski (2013a), "Modeling and Analysis of Thermal Phenomena Governing Bubble Growth and Collapse in Subcooled Boiling", Proc. American Nuclear Society 2013 National Student Conference, MIT, Boston, Massachusetts.*

H. Jiao, S.P. Antal and M.Z. Podowski (2013b), "Modeling and Analysis of Interfacial Heat Transfer Phenomena in Subcooled Boiling along PWR Coolant Channels", Paper#587, Proc. 15th Int. Topical Meeting on Nuclear Reactor Thermalhydraulics (NURETH-15), Pisa, Italy.*

N. Kurul and M. Z. Podowski (1991) "On the Modeling of Multidimensional Effects in Boiling Channels", ANS Proc. National Heat Trans. Conf., Minneapolis, MN.

M.Z. Podowski (2009), "On the Consistency of Mechanistic Multidimensional Modeling of Gas/Liquid Two-Phase Flows", Nucl. Eng. and Design, 239, pp.933-934.

M.Z. Podowski (2012a), "Toward Mechanistic Modeling of Boiling Heat Transfer", Nuclear Engineering and Technology, V44, No.8, pp.1-8.*

M.Z. Podowski (2012b), "Mechanistic Modeling of Boiling Heat Transfer", Proc. Embedded Topical Meeting: Advances in Thermal-Hydraulics, 2012 ANS Winter Meeting, San Diego, CA, pp.1-5.*

M.Z. Podowski and D.R. Shaver 2013), "Recent Advancements in Multidimensional Modeling of Two-Phase Flow and Heat Transfer In Reactor Fuel Assemblies", Proc. International Seminar on Subchannel Analysis, CFD Modeling and Verification, CHF Experiments and Benchmarking, Xi'an, China.*

D.R. Shaver, S.P. Antal, M.Z. Podowski and D.H. Kim (2010), "Direct Steam Condensation Modeling for a Passive PWR Safety System", Proc. CFD4NRS-3, Washington, D.C., USA.

D.R. Shaver, S.P. Antal, and M.Z. Podowski (2012), "Development, Testing, and Validation of a Multidimensional Model of Subcooled Boiling", ANS Transactions, 2012 Winter Meeting, San Diego, CA, pp. 1366-1368.*

D.R. Shaver, S.P. Antal, and .Z. Podowski (2013a), "Modeling and Analysis of Interfacial Heat Transfer Phenomena in Subcooled Boiling along PWR Coolant Channels", Paper #586, Proc. 15th Int. Topical Meeting on Nuclear Reactor Thermalhydraulics (NURETH-15), Pisa, Italy.*

D.R. Shaver, S.P. Antal, and .Z. Podowski (2013b), "Multiscale Modeling of Two-phase Flow and Interfacial Heat Transfer Phenomena in Subcooled Boling", Proc. Int. Conference on Multiphase Flow, Jeju, South Korea.*

D. R. Shaver, M. Z. Podowski (2013c), "A Fundamental Model for Predicting Bubble Size in Diabatic Multiphase Flows", ANS Transactions, 2013 ANS Winter Meeting and Nuclear Technology Expo, Washington, DC.*

D. R. Shaver, M. Z. Podowski (2013), "A Mechanistic Model of Subcoled Boiling in Nuclear Reactors", Nucl. Eng. Des., in preparation.*

D. R. Shaver and M. Z. Podowski (2013a), "Model Development for Large-Scale Nuclear Power Reactor Simulations", Proc. American Nuclear Society 2013 National Student Conference, MIT, Boston, Massachusetts.*

S.Z. Rouhani (1966), "Vid measurements in the Regions of Subcooled and Low-Quality Boiling", AE-239, Stockholm, Sweden.

B.M. Waite, D.R. Shaver and M.Z. Podowski (2012), "Multidimensional Analysis of Flow through Sudden Expansions and Contractions in Pipes", ANS Transactions, 2012 Winter Meeting, San Diego, CA, pp. 1336-1368.*

B.M. Waite, D.R. Shaver, M. Z. Podowski (2013a), "Multidimensional Analysis of Local Flow Obstacles in Nuclear Reactors", Proc. American Nuclear Society 2013 National Student Conference, MIT, Boston, Massachusetts.*

B.M. Waite, D. R. Shaver, M. Z. Podowski (2013b), "Prediction of Pressure Drop and Heat Transfer around Flow Obstructions", ANS Transactions, 2013 ANS Winter Meeting and Nuclear Technology Expo, Washington, DC.*

S.K. Wang, S.J. Lee, O.C. Jones, and R.T. Lahey Jr. (1987), "3-D Turbulence Structure and Phase Distribution Measurements in Bubbly Two-Phase Flows", Int. J Multiphase Flow, Vol. 13 No.3.*

M. D. Zimmer, D. R. Shaver, M. Z. Podowski (2013), "An Analysis of Multidimensional Models of Turbulent Flow in Nuclear Reactors", Proc. American Nuclear Society 2013 National Student Conference, MIT, Boston, Massachusetts.*

INVITED LECTURES AND SEMINARS, 2012-13

Plenary Lecture: M.Z. Podowski, ""Recent Advancements in Multidimensional Modeling of Two-Phase Flow and Heat Transfer In Reactor Fuel Assemblies", International Seminar on Subchannel Analysis, CFD Modeling and Verification, CHF Experiments and Benchmarking, Xi'an, China, August 2-4, 2013.

Invited Lecture: M.Z. Podowski, "Importance of Coupling between Modeling and Computational Issues in Multiphase Flow and Heat Transfer Simulations", Two-Phase Flow Workshop, North Carolina State University, May 2, 2013.

Invited Seminar Speaker: M.Z. Podowski, "Toward the Development of a Virtual Reactor: Modeling and Computational Issues in Multiphase Flow and Heat Transfer", Department of Nuclear Engineering, University of Michigan, Ann Arbor, MI, December 7, 2012.

Opening Lecture: M.Z. Podowski, "Challenges in Computational Modeling of Multiphase Flow and Heat Transfer", International Computational Modeling Validation Conference, Sydney, Australia, January 14, 2012.

Keynote Lecture: M.Z. Podowski, "Validation of Computational Modeling of Multiphase Flow and Heat Transfer", International Computational Modeling Validation Conference, Sydney, Australia, January 15, 2012.